Performance Evaluation of Strain Gauge Printed Using Automatic Fluid Dispensing System on Conformal Substrates

Rd. Khairilhijra Khirotdin[1,a] , Mohamad Faridzuan Ngadiron[1,b] , Muhammad Adzeem Mahadzir[1,c] And Nurhafizzah Hassan[2,d]

[1]Faculty of Mechanical and Manufacturing Engineering, University of Tun Hussein Onn Malaysia, 86400 Parit Raja, Batu Pahat, Johor, Malaysia
[2]Faculty of Engineering Technology, University of Tun Hussein Onn Malaysia, 86400 Parit Raja, Batu Pahat, Johor, Malaysia

Corresponding author: [a]khairil@uthm.edu.my, [b]mfaridzuann@gmail.com, [c]adzeemmahadzir@gmail.com, [d]hafizzah@uthm.edu.my

Abstract. Smart textiles require flexible electronics that can withstand daily stresses like bends and stretches. Printing using conductive inks provides the flexibility required but the current printing techniques suffered from ink incompatibility, limited of substrates to be printed with and incompatible with conformal substrates due to its rigidity and low flexibility. An alternate printing technique via automatic fluid dispensing system is proposed and its performances on printing strain gauge on conformal substrates were evaluated to determine its feasibility. Process parameters studied including printing speed, deposition height, curing time and curing temperature. It was found that the strain gauge is proven functional as expected since different strains were induced when bent on variation of bending angles and curvature radiuses from designated bending fixtures. The average change of resistances were doubled before the strain gauge starts to break. Printed strain gauges also exhibited some excellence elasticity as they were able to resist bending up to 70° angle and 3 mm of curvature radius.

1. Introduction

Strain gauge is a sensor that detects the changes of electrical resistance as it undergoes deformation in order to measure strain and used in monitoring shape, strain, stress and pressure of a system. The interest has rapidly increased especially in the smart textile application [1] which the strain gauge needs to be flexible and rigorous to handle typical stresses caused by human body motion [2]. Conventional strain gauges are unsuitable due to its rigidity and low flexibility nature [3] exhibited from metallic foil fabrication method. An alternative of conventional strain gauge are digital component fabricated using printing technologies with the aid of conductive ink also known as printed electronics (PE). PE is more flexible and bendable when compared to conventional electronic product and sensor [4] because the conductive ink is formulated using elastomers that have metallic fillers [5]. Silver and copper conductive ink are frequently adapted by researchers in experimenting printed electronics due to its availability in market [6]. Silver ink is used in this experiment because the conductivity properties are slightly better than copper ink [7].

There are a lot of reports regarding the usage of conductive ink in fabricating printed strain gauge on planar substrates such as glass [5], printed circuit board [6], polyethylene terephthalate (PET) [7]

and paper [8] via inkjet, flexography, aerosol and gravure printing respectively. There are also reports on other type of sensors fabricated using printing technologies besides strain gauge such as humidity sensors via rotogravure printing [9], RFID tags via inkjet printing [10], electrochemical sensors via rotogravure printing [11], gas sensors via screen printing [12] and organic thin film transistors via inkjet printing [13][14]. However, most of these printing techniques only capable of printing on planar substrates and some of these techniques suffer from clogging as well as limited type of materials to be printed with [15].

In contrast, fluid dispensing system which equipped with three dimensional coordinate axes is independent of standoff height and not relying to the surface tension between substrates allowing it to be used on numerous substrates [16]. It is also used air over dispensing driving mechanism to force the material out through the nozzle [17]. The system has been widely used in electronic industries especially in solder paste machine and surface mount technology [18]. Currently, there are no reports found on the used of fluid dispensing system in fabricating a functional electronics structure and the potential of the system has not been thoroughly explored especially on printing of electronics structure on non-planar substrates. Thus, an investigation is needed to evaluate the performance of the electronics structure printed using the aforementioned system on non-planar substrates. By realizing this, it will open up a new scale of target market especially in the field of wearable electronics application (smart textiles) or structural and health monitoring system.

2. Methodology

The methodology of the study are summarized in Fig. 1.

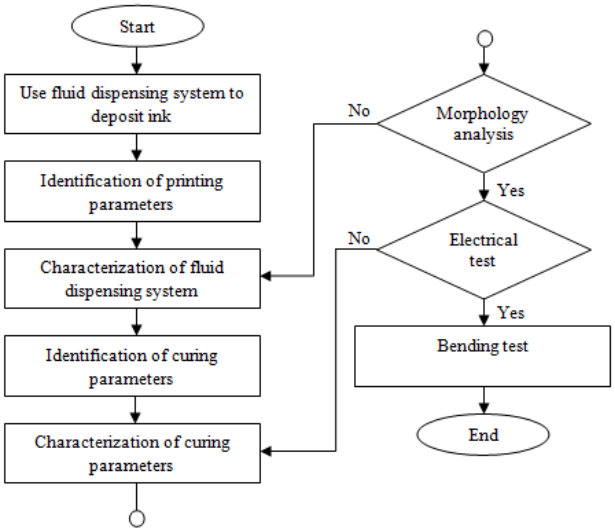

Fig. 1. The flowchart of experiment conducted.

2.1 Deposition of ink and curing process

Fisnar bench top robot (model F4200N.1) shown in Fig. 2. is used as a fluid dispensing system to print the conductive ink on non-planar substrates via fabric and curvature substrates. The electronics structure printed is a strain gauge sensor and it was modeled first using suitable drafting tool (AutoCAD) and its detail dimensions are shown in Fig. 3. The total length of the strain gauge is 221.42 mm long with a 2 mm width of track. For fabric substrate, the printing speed was varied between 3 to 5 mm/s while deposition height was varied from 0.5 mm to 1.5 mm. For curvature substrate, printing speed and pressure were varied from 4 to 6 mm/s and 0.6 to 0.8 bar. The curing process is performed using a combination of Direct Light Projector (DLP) and hot plate for fabric substrate [19] while for curvature substrate oven curing is used to reduce the percentage of unwanted

material in conductive ink in order to get the best electrical conductivity properties of the ink tracks. Curing temperatures were varied from 110°C to 150°C for DLP and hot plate while for oven; the curing temperatures were varied from 140^{o} to 180°C. The curing times were also varied from 15 to 45 minutes for the DLP and hot plate while for the oven; the curing times were varied from 30 to 50 minutes. Table 1 below shows the variation of printing and curing parameters selected and a total of nine samples were obtained for each substrate from the simplification method made using Taguchi method.

Fig. 2. FISNAR benchtop robot (model F4200N.1)

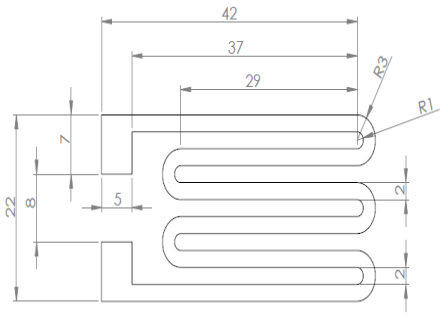

Fig. 3. Dimension of the strain gauge sensor (units in mm).

Table 1. Tabulated variation of printing and curing parameters selected for the study.

Experiment (Fabric substrate)	Printing Speed (mm/s)	Deposition Height (mm)	Temperature (^{o}C)	Time (min)	Experiment (Curvature substrate)	Printing Speed (mm/s)	Printing Pressure (bar)	Temperature (^{o}C)	Time (min)
1	3	0.5	110	15	1	4	0.6	140	30
2	3	1.0	130	30	2	4	0.7	160	40
3	3	1.5	150	45	3	4	0.8	180	50
4	4	0.5	110	45	4	5	0.6	160	50
5	4	1.0	130	15	5	5	0.7	180	30
6	4	1.5	150	30	6	5	0.8	140	40
7	5	0.5	110	30	7	6	0.6	180	40
8	5	1.0	130	45	8	6	0.7	140	50
9	5	1.5	150	15	9	6	0.8	160	30

2.2 Material and substrate

The conductive ink used is silver epoxy based ink (model AG806) and direct usage of the ink is not possible due to high solid fraction thus an adjustment of viscosity via dilution with Toluene solvent is necessary. The fabric material used is made of lycra and since the aim is to embed sensor on cloth, lycra material is much suitable because it is a type of compression wear where under compression it clings strict to the skin and quite literally squeezing the muscles below without irritation hence helps to increase the sensor sensing capabilities. Recycled aluminium tin cans are cut into aluminum sheets that are pasted on the surface of aerofoil shape mandrels to mimic the curvature metal substrate. The fabric and curvature substrate are both shown in Fig. 4 and 5.

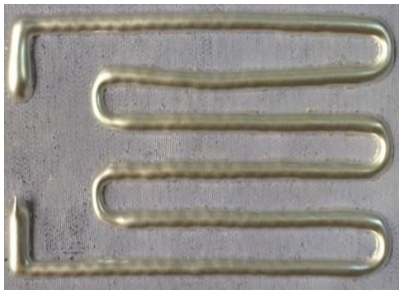

Fig. 4. Lycra substrate

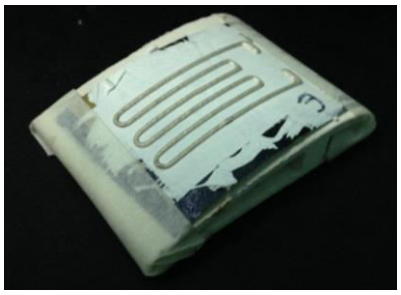

Fig. 5. Curvature substrate

2.3 Measurement

Analysis of the strain gauge printed is consisted of the measurement of the line width and thickness of the ink track using an optical microscope and its electrical properties via IV test. The cross-sectional area of the ink track and its total length were determined to calculate the resistivity. Functional tests are performed in the form of bending and curvature test which the used of customized bending [19] and curvature jigs are employed as shown in Fig. 6 and 7. The purpose of these tests is to analyse the electro-mechanical response when the strain gauge is subjected to bending deformation. The microstructure grain bonding between particles of the ink track was determined using the Scanning Electron Microscope (SEM) and the particles total composition was analyzed using Energy Dispersive X-Ray Spectroscope (EDS).

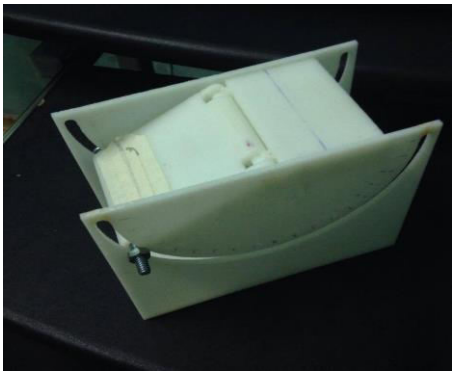

Fig. 6. Customized bending jig.

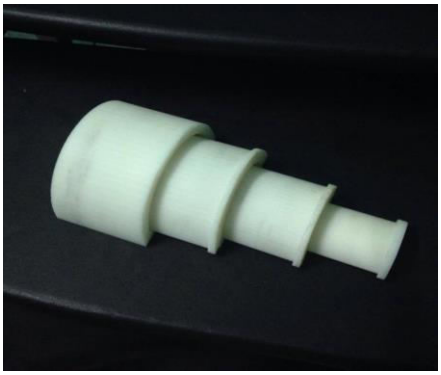

Fig. 7. Customized curvature jig.

3. Result

3.1 Morphology analysis

Tabulated results of the morphological and electrical analysis are shown in Table 2 and 3 for both substrates. The purpose of morphological analysis is to identify the relationship between variations of printing parameters with the fabricated strain gauge ink track size. Cross-sectional area and the total length of the strain gauge were then used to calculate the resistivity. It was found that the electrical properties of the strain gauge is strongly affected by the curing parameters while the ink track size of the strain gauge only plays a minor factor.

Fig. 8 shows the relationship between printing speed parameters with the line with and line thickness for different ink deposition height of the printed strain gauge ink track on fabric substrate. It was observed that all results shown a constant decreased in line width as the printing speed increased. This is due to the increase in printing speed lowered the volume of the ink being dispensed and

Table 2. Morphological and electrical properties for sample printed on fabric substrates.

Sample	Line width (mm)	Line thickness (mm)	Cross-sectional area (mm^2)	Length (mm)	Resistance (Ω)	Resistivity (Ωm)	Conductivity (S/m)
1	2.359	0.795	1.875	215.8	8.31	7.222E-05	13846.67
2	2.228	0.793	1.767	215.1	2.16	1.774E-05	56374.02
3	2.176	0.797	1.734	214.9	1.53	1.235E-05	80981.79
4	2.184	0.754	1.647	214.9	1.65	1.264E-05	79098.62
5	2.043	0.749	1.530	214.2	1.94	1.386E-05	72160.24
6	1.850	0.747	1.382	213.3	2.21	1.432E-05	69823.95
7	2.031	0.732	1.487	214.2	1.64	1.139E-05	87834.14
8	1.785	0.721	1.287	212.9	2.09	1.263E-05	79160.20
9	1.632	0.735	1.200	212.2	2.37	1.340E-05	74629.01

Table 3. Morphological and electrical properties for sample printed on curvature substrates.

Sample	Line width (mm)	Line thickness (mm)	Cross-sectional area (mm^2)	Length (mm)	Resistance (Ω)	Resistivity (Ωm)	Conductivity (S/m)
1	1.965	0.672	1.320	213.8	2.48	1.532E-05	65294.26
2	2.034	0.839	1.707	214.2	1.12	8.924E-06	112054.10
3	2.239	1.082	2.423	215.2	3.68	4.143E-05	24138.10
4	1.852	0.521	0.965	213.3	1.89	8.551E-06	116941.60
5	1.921	0.642	1.233	213.6	1.24	7.159E-06	139677.80
6	2.187	0.885	1.935	214.9	2.21	1.990E-05	50248.47
7	1.705	0.482	0.822	212.5	3.62	1.400E-05	71438.12
8	1.895	0.574	1.088	213.5	2.08	1.060E-05	94354.49
9	1.944	0.812	1.579	213.7	1.46	1.078E-05	92734.22

shortened the time of the ink to disperse on the substrate. When compared between the three of them, the line width itself showed a constant decreased when the deposition height increased. Bigger ink deposition height is actually disrupted the continuity of the ink's flows thus resulted in decreasing the volume of the ink dispersed on the substrate. Meanwhile, the line thickness for the three different deposition heights showed only a slight decreased as the printing speed increased. It concludes that the line thickness is not heavily affected by the ink deposition height and the ink deposition heights only play a small role in determining the thickness of the ink track.

Fig. 9 shows the established relationship between the line width and thickness with printing speed for variation of printing pressures for the printed strain gauge ink track on curvature substrate. All results shown a constant decreased in line width as the printing speed increased. This is due to similar reason as deposition height. When compared between the three of them, the line width of ink track showed a constant increased when the printing pressure increased. Higher printing pressure allowed more volume of the ink to dispense on substrate. Besides, the line thickness for three different printing pressures as well showed only a slight decreased as the printing speed increased. Similar impact occurred from the effect of deposition height which the line thickness is not heavily affected by the printing pressure and plays only a small part in determining the thickness of the ink track.

3.2 Electrical analysis

The relationship established between the resistance and curing time for different curing temperatures is illustrated in Fig. 10. Each curing temperature result showed a constant decreased in resistance as the curing time increased. This is due to the increase in curing time provide more process time for the binder in the ink to react to the heat energy supplied and evaporated. When compared between the three different curing temperatures, the resistance obtained showed a constant decreased when the curing temperature increased. This is because the increase in curing temperature increased

the heat energy supplied to the ink thus increasing the activity of the binder to evaporate more in a faster rate. In the mean time, Fig. 11 shows the relationship established between the conductivity of the ink track with the curing time for different curing temperatures. Conductivity is inversely proportional to the volume resistivity of the ink. The conductivity should increase as the curing time increase for each temperature. However, the only result that follows this trend is when the curing temperature is at 110°C while when the temperature is at 130°C, the conductivity attained shows a decrease at a curing time of 30 minutes. When compared between the cross-sectional areas of the three samples, sample with curing time of 30 min has the largest cross-sectional area and the longest length. The heat distribution between particle in the ink track is the lowest thus affecting the conductivity of the ink track. For temperature of 150°C, the conductivity at 45 minutes showed a slight decreased due to the cumulative heat energy supplied during the curing process was too high. Instead of evaporating the binder, it turned into impurities thus affecting the particle bonded and increasing the resistivity of the ink track. For this situation, the samples are considered over cured.

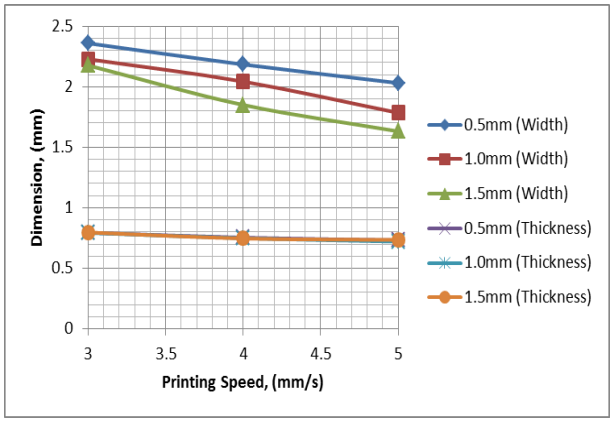

Fig. 8. Changes of the ink track line width and thickness as the printing speed increased for different deposition heights on fabric substrate.

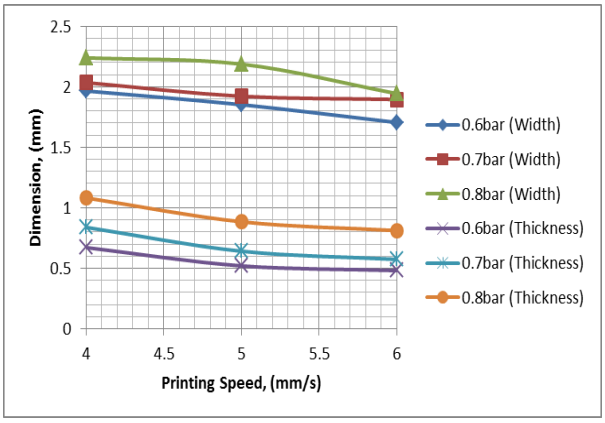

Fig. 9. Changes of the ink track line width and thickness as the printing speed change for different printing pressure on curvature substrate

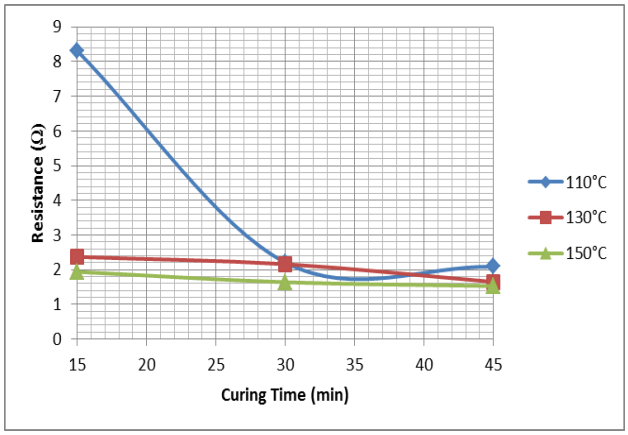

Fig. 10. Changes of resistance properties of the ink track as the curing parameters change on fabric substrate.

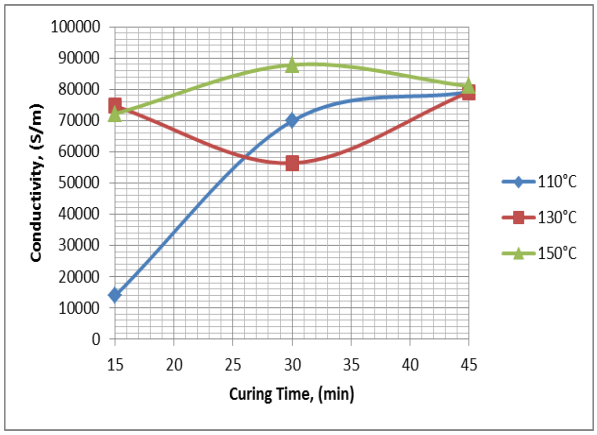

Fig. 11. Changes of electrical conductivity properties of the ink track as curing parameters change on fabric substrate.

Silver particles bonded was analyzed using SEM and shown in Fig. 12 (a) and (b) for sample 1 and sample 3 respectively. For sample 1, the bonds between silver particles are spreaded apart from each

other and larger gaps are observed than sample 3. The gap (circle in white) between silver particles obstructed the movement of electrons between silver particles thus increased the total electrical resistance of the ink track. This explain the reason why sample 3 has lower electrical resistance than sample 1. In addition, EDX analysis was also conducted on both samples to obtain the total composition of the ink track. Only two elements were traced from both samples that is silver and carbon. Carbon element is the leftover from the unevaporated binder during curing process. A 80.46% and 19.54% of silver and carbon particles contents were traced for sample 1 while 86.33% and 13.67% of silver and carbon particles contents were indicated for sample 3. The higher percentage of silver particles also explains that more electron transmitted through the particles resulted in lower electrical resistance value.

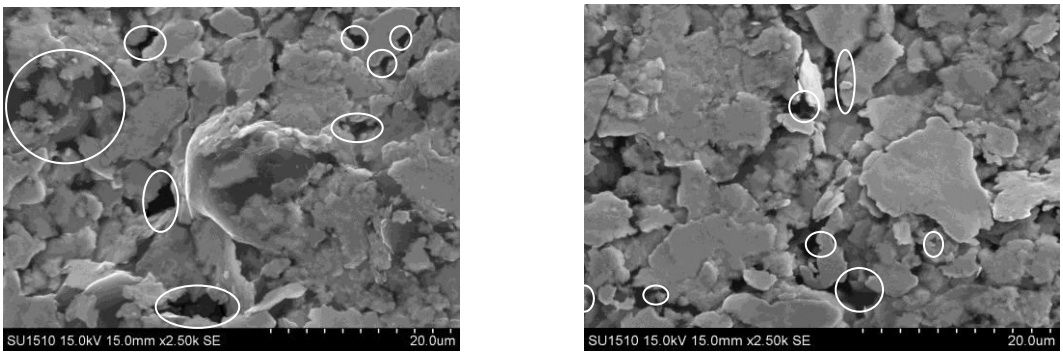

(a) (b)

Fig. 12. SEM image of silver particles bonding arrangement for (a) sample 1 (b) sample 3 (Gaps denoted as white circle)

The relationship established between resistance and curing time for different curing temperature is shown in Fig. 13 for curvature substrate. Resistance should decrease as the curing temperature and curing time increased [20]. This is due to the increase in curing time given more process time for binder to evaporate more as the heat energy supplied is increased. However, the only result following the trend is at curing temperature of 140°C. For temperature at 160°C, the sample followed the trend but the sample reached over-cured state at the curing time of 50 minutes. As for temperature at 180°C, the sample reached over-cured state at the curing time of 40 and 50 minutes. The relationship between the conductivity and curing time for different curing temperature is also depicted in Fig. 14. Conductivity is affected by the volume resistivity of the ink track. The conductivity should increase as the curing time increase for all temperatures. However, the only result that follow this trend is at curing temperature of 160°C. For temperature at 140°C, the conductivity shows a decrease at curing time of 40 minutes. When compared between the cross-sectional area of the three samples, sample with curing time of 40 minutes has the largest cross-sectional area with the longest length. The heat distribution between particles is the lowest thus affecting the conductivity. For temperature at 180°C, the conductivity is decreased as the curing time increased. This is because the sample has already over cured. The longer the samples exposed to heat, the more impurities are produced. The sample is too dry which result in crack and gaps. It disrupted the path for electrons to flow properly thus higher resistance is obtained.

Silver particle bonded of the ink track was analyzed using SEM and shown in Fig.15 (a) and (b) for sample 3 and sample 2 respectively. The bond between silver particles for sample 3 is spreaded apart from each other and the gaps (circle in white) observed between the particless are larger than sample 2. The gap between the silver particle obstructed the movement of electrons between silver particle thus increased the total electrical resistance of the strain gauge. This explain the reason why sample 2 has a lower electrical resistance value than sample 3. An EDX analysis was also performed on both

samples to obtain the composition of ink track. Only two elements were traced from both samples that is silver and carbon. Carbon element in the ink track is the leftover of the binder that did not evaporate and left as impurities from overcuring during the curing process. Sample 3 shows 83.55% of silver particle and 16.45% of carbon particles while sample 2 shows 92.23% of silver particles and 7.77% of carbon particles respectively. The larger percentage of silver particles also explains that more electrons could be transmitted through the particles resulted in lower resistance value.

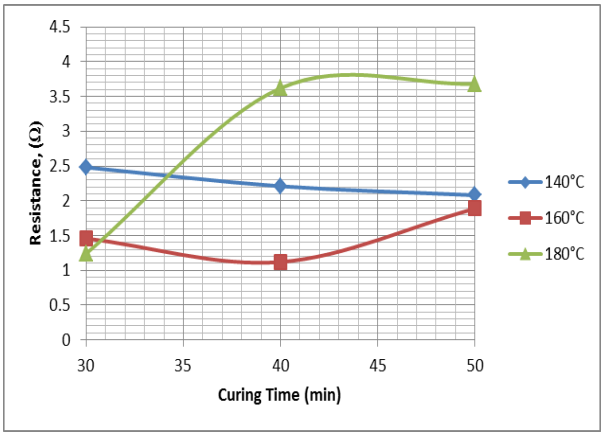

Fig. 13. Changes of resistance on curvature substrates as the curing parameters varies.

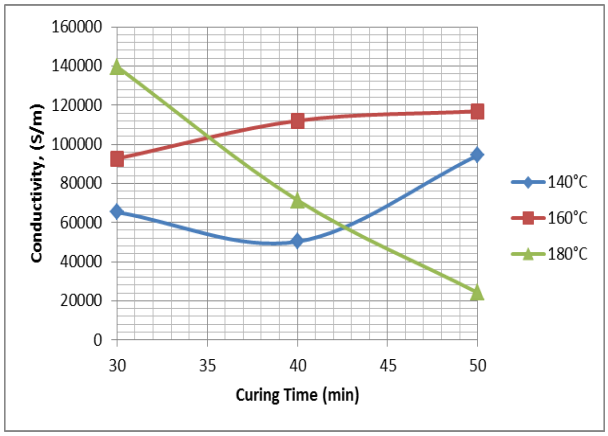

Fig. 14. Changes of conductivity properties on curvature substrates as the curing parameters varies.

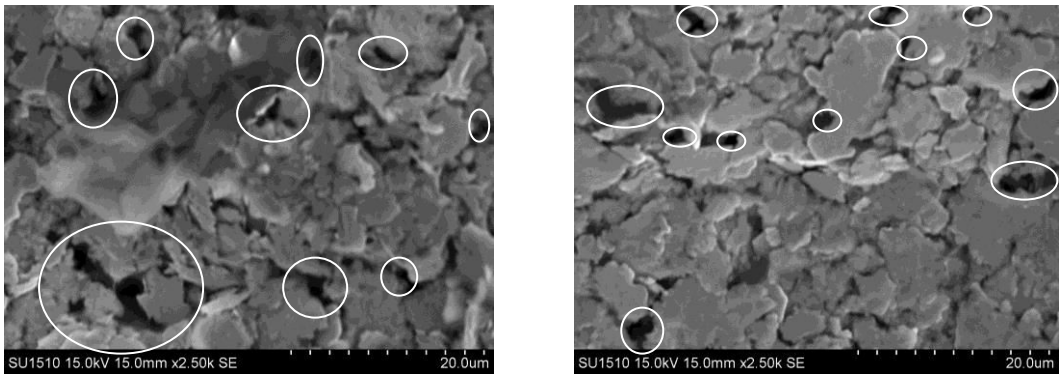

(a) (b)

Fig. 15. SEM image of silver particles bonding arrangement for (a) sample 3 (b) sample 2 (Gaps denoted as white circle)

3.3 Performance evaluation

Table 4 shows the results of bending test conducted for all samples. It was found that the resistance of the ink track increased when the bending angles applied are increased as shown in Fig. 16. This is because as the bending angle increased, the particles bonded in the ink are started to move far apart thus increased the resistance of the ink track [19]. The elasticity value for each sample is different. Sample 5 exhibits the best elasticity value because the printing and curing parameters used are at its medium range thus confirming the optimum parameters for printing and curing in fabricating the strain gauge.

In Table 4 as well shows the results of bending test conducted for all samples printed on curvature substrate. As the bending radius decreased, the strain induced on the strain gauge increased. Fig. 17 shows the changes of resistance for all samples printed on curvature substrates at different bending radius. Sample 1, 2, 3 and 6 have a very low elasticity properties as it could not be bent even at the biggest radius of curvature (5 cm). As the strain induced is increased, the resistance of the strain gauge is increased. This is because as the strain increased, the distance between particles are far apart thus increased the resistance value of the strain gauge. Sample 7 shows excellence elasticity due to the lowest cross-sectional area compared to other samples.

Table 4. Tabulated results of change in resistances for all samples (fabric and curvature substrates) as it undergoes bending test

Sample (Fabric substrate)	Initial Resistance (Ω)	Final Resistance (Ω)	Increment (%)	Failure Angle (°)	Sample (Curvature substrate)	Initial Resistance (Ω)	Final Resistance (Ω)	Increment (%)	Failure (cm)
1	8.31	10.13	121.9013	60	1	2.48	2.48	-	5
2	2.16	3.62	167.5926	50	2	1.12	1.12	-	5
3	1.53	2.28	149.0196	40	3	3.68	3.68	-	5
4	1.65	3.50	212.1212	50	4	1.89	2.14	113.2275	4
5	1.94	15.20	783.5052	80	5	1.24	3.84	309.6774	3
6	2.21	4.20	190.0452	60	6	2.21	2.21	-	5
7	1.64	6.42	391.4634	70	7	3.62	9.31	257.1823	2
8	2.09	3.21	153.5885	40	8	2.08	3.17	152.4038	3
9	8.37	3.99	47.6702	50	9	1.46	2.82	193.1507	3

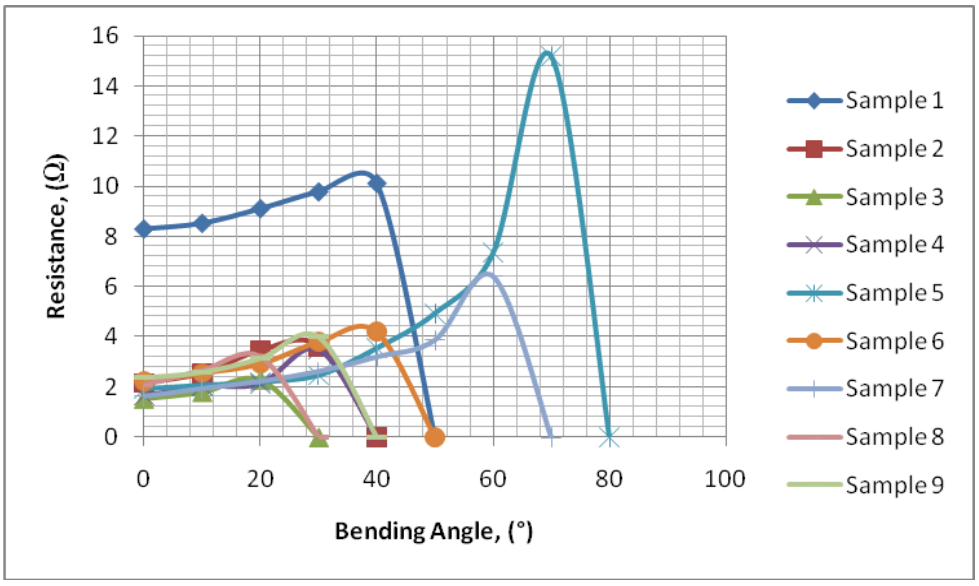

Fig. 16. Resistance changes for all samples at different bending angles.

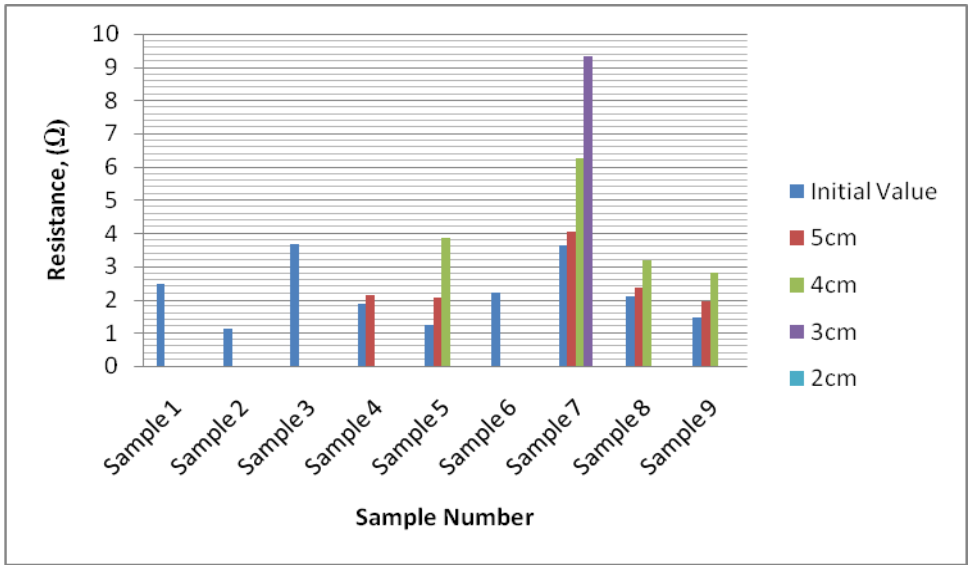

Fig. 17. Changes in resistance for all samples printed on curvature substrates at different bending radius

4. Conclusion

Conductive ink tracks printed on fabric and curvature substrates were evaluated by bending test in order to determine its reliability in performing real life application. The bending test results found to be as expected which the strain gauge resistance increased when underwent bending deformation. The changes of resistance in printed strain gauge shows that it could detect different strain induced and it proves to be capable of functioning well in real life application. Thus, it concludes that automatic fluid dispensing systems is capable of fabricating a functional electronic structure on non-planar substrates. The average resistance increment for strain gauge printed on fabric substrates are doubled from its original value. Sample 5 which considered as the most flexible substrate has maximum bending that is 70° angle and it maximum resistance value increased up to seven times of its initial resistance value. For curvature substrate, the average resistance increment is doubled as well. Sample 7 has the highest elasticity value among other samples as it could be bent up to 3 mm bending radius with maximum increment of resistance value up to 2.5 times of its original value. Thus, the objective to determine a maximum bending track is achieved showing that this evaluation study of performance of simple electronic structure printed using automatic fluid dispensing system is a success.

Acknowledgement

The authors gratefully acknowledge the support to the Ministry of Higher Education of Malaysia and University of Tun Hussein Onn Malaysia under the Research Acculturation Grant Scheme awarded (RAGS-R052) and giving the opportunity to attend and present at this conference

References

[1] Stoppa M and Chiolerio A 2004 Wearable Electronics and Smart Textiles: A Critical Review *Sensors* **14**(7) 11957–11992

[2] Nesenbergs K and Selavo L 2015 Smart Textiles for Wearable Sensor Networks : Review and Early Lessons IEEE International Symposium on Medical Measurement and Application (MeMeA)

[3] Arruda L 2007 On the Simulation of Flexible Circuits Boards EMPC2007 6th European Microelectronics and Packaging Conference 984-989

[4] Khan S, Lorrenzelli L, Dahiya R S 2015 Technologies for Printing Sensors and Electronics Over Large Flexible Substrates : A Review IEEE *Sensors Journal* **15**(6) 3164–3185
[5] Inoue M, Tada Y, Muta H, Hayashi Y, Tokumaru T 2012 Development of Highly Conductive Inks for Smart Textiles 14th International Conference on Electronic Materials and Packaging (EMAP)
[6] Abhinav K V, Rao R, Karthik V K, Singh S P 2015 Copper Conductive Inks: Synthesis and Utilization in Flexible Electronics *RSC Advances* **5**(79) 63985–64030
[7] Halonen E, Viiru T, Ostman K, Cabezas A, Mantysalo M 2013 Oven Sintering Process Optimization for Inkjet-Printed Ag Nanoparticle Ink *IEEE Transactions on Components, Packaging and Manufacturing Technology* **3**(2), 350-356
[8] Lakshmi R, Debeda H, Defour I, Lucat C 2010 Force Sensor Based of Screen-printed Cantilevers IEEE *Sensors* **10** 1133–1137
[9] Shi H, Ikexawa S, Ueda T 2011 A Novel Method for Evaluating Triaxial Strain Gages used in Printed Circuit Board Assemblies (PCBA) Strain Monitoring IEEE *Sensors* 1697–1700
[10] Moorthi A, Narakathu B B, Reddy A S G, Eshkeiti A, Bohra H, Atashbar M Z 2012 A Novel Flexible Strain Gauge Sensor Fabricated using Screen Printing 6th International Conference on Sensing Technology 765–768
[11] Maddipatla D, Narakathu B B, Guruva S, Avuthu R, Emamian S, Eshkeiti A 2015 A Novel Flexographic Printed Strain Gauge on Paper Platform IEEE *Sensors* 8–11
[12] Reddy A S G, Narakathu B B, Atashbar M Z, Rebros M, Rebrosova E, Bazuin B J, Joyce M K, Fleming P D, Pekarovicova A 2011 Printed Capacitive Based Humidity Sensors on Flexible Substrates *Sen. Let*. **9** 869–871
[13] Li J, An B, Qin J, Wu Y 2011 Nano Copper Conductive Ink for RFID Application International Symposium on Advanced Packaging Materials (APM) 91–93
[14] Reddy A S G, Narakathu B B, Atashbar M Z, Rebros M, Rebrosova E, Joyce M K 2011 Gravure Printed Electrochemical Biosensor *Proc. Eng*. **25** 956-959
[15] Laschi S, Palchetti I, Mascini M 2006 Gold-based Screen-printed Sensor for Detection of Trace Lead *Sens. and Act. B* **114** 460–465
[16] Nguon B and Jouaneh M 2004 Design and Characterization of A Precision Fluid Dispensing Valve *International Journal of Advanced Manufacturing Technology* **24**(3-4) 251–260
[17] Dixon D 2009 Time Pressure Dispensing: White Papers Universal Instruments
[18] Hashemi M and Chen X B 2008 Theoretical Investigation Into The Performance of the Rotary-Screw Fluid Dispensing Process *Transaction of the CSME/de la SCGM* **32**(3-4) 325–332
[19] Khirotdin R K, Cheng T S, Mokhtar K A 2016 Printing of Conductive Ink on Textile using Silkscreen Printing *ARPN Journal of Engineering and Applied Sciences* **11**(10), 6619-6624
[20] Khirotdin R K, Zakaria D A, Mohadhir M 2016 Printing and Curing Silver Conductive Ink Tracks from Modified On-shelf Inkjet Printer on Fabric *International Journal of Mechanical & Mechatronics Engineering IJMME-IJENS* **16**(6), 50-56